1000-0569/2012/028(02)-0483-94 *Acta Petrologica Sinica* 岩石学报

内蒙古道郎呼都格地区 A 型花岗岩年代学、地球化学及地质意义*

解洪晶[1,2] 武广[3]** 朱明田[4] 刘军[3] 张连昌[4]
XIE HongJing[1,2], WU Guang[3]**, ZHU MingTian[4], LIU Jun[3] and ZHANG LianChang[4]

1. 中国科学院广州地球化学研究所矿物学与成矿学重点实验室,广州 510640
2. 中国科学院研究生院,北京 100049
3. 中国地质科学院矿产资源研究所,北京 100037
4. 中国科学院地质与地球物理研究所矿产资源研究重点实验室,北京 100029
1. *Key Laboratory of Mineralogy and Metallogeny, Guangzhou Institute of Geochemistry, Chinese Academy of Sciences, Guangzhou* 510640, *China*
2. *Graduate School of Chinese Academy of Sciences, Beijing* 100049, *China*
3. *Institute of Mineral Resources, Chinese Academy of Geological Sciences, Beijing* 100037, *China*
4. *Key Laboratory of Mineral Resources, Institute of Geology and Geophysics, Chinese Academy of Sciences, Beijing* 100029, *China*
2011-08-05 收稿, 2011-10-25 改回.

Xie HJ, Wu G, Zhu MT, Liu J and Zhang LC. 2012. Geochronology and geochemistry of the Daolanghuduge A-type granite in Inner Mongolia, and its geological significance. *Acta Petrologica Sinica*, 28(2):483–494

Abstract The K-feldspar granite intrusion from Daolanghuduge, Inner Mongolia, is located in the Bainaimiao arc of the northern margin of the North China Craton (NCC). The SHRIMP analyses of zircons from the intrusion yield a weighted mean $^{206}Pb/^{238}U$ age of 139.6±1.7Ma. The intrusion is characterized by high SiO_2 contents (75.79% ~78.07%), high alkali contents (K_2O+Na_2O = 7.39% ~8.29%) but low CaO contents (0.22% ~0.59%). The K-feldspar granite is marked by a "sea-gull" pattern of REE distribution with a δEu ranging from 0.03 to 0.12, showing a relatively significant negative Eu anomaly. These rocks are enriched in Ga (21.2×10^{-6} ~26.6×10^{-6}), Zr (173×10^{-6} ~417×10^{-6}), Nb (32.3×10^{-6} ~42.4×10^{-6}) and Y (24.6×10^{-6} ~53.9×10^{-6}) but depleted in Sr (14×10^{-6} ~44×10^{-6}) and Ba contents (18×10^{-6} ~211×10^{-6}), and exhibit remarkably negative Ba, Sr, P, Eu and Ti anomalies on the primitive mantle-normalized trace element diagram. All these characteristics resemble A-type granites which originated from the partial melting of felsic crust under high temperature and low pressure conditions and the subsequent fractional crystallization of feldspar, titanite, etc. Combined with regional tectonic evolution, we suggest that the K-feldspar granite formed in an intraplate extensional setting. The northern margin of the NCC went through a transitional tectonic regime from compression to extension during Late Mesozoic. Under this tectonic regime, the upwelling asthenosphere provided enhanced heat flux and triggered the partial melting of the overlying felsic crust and then produced the Daolanghuduge K-feldspar granite intrusion.
Key words A-type granite; Zircon SHRIMP U-Pb age; Geochemistry; Daolanghuduge intrusion; Inner Mongolia

摘 要 道郎呼都格钾长花岗岩体位于华北克拉通北缘白乃庙构造带。SHRIMP 锆石 U-Pb 定年获得 139.6±1.7Ma 岩体侵位年龄。岩体富硅(SiO_2 =75.79% ~78.07%)、富碱(K_2O+Na_2O =7.39% ~8.29%)、贫钙(CaO =0.22% ~0.59%);稀土配分曲线呈现"海鸥式"分布特征,显示强烈的 Eu 负异常(δEu =0.03 ~0.12);微量元素特征显示具有较高 Ga(21.2×10^{-6} ~26.6×10^{-6})、Zr(173×10^{-6} ~417×10^{-6})、Nb(32.3×10^{-6} ~42.4×10^{-6})和 Y(24.6×10^{-6} ~53.9×10^{-6})含量,较低的 Sr(14×10^{-6} ~44×10^{-6})、Ba(18×10^{-6} ~211×10^{-6})含量,在微量元素原始地幔标准化蛛网图上显示明显的 Ba、Sr、P、Eu 和 Ti 的负异常。以上特征表明道郎呼都格钾长花岗岩为 A 型花岗岩,为高温低压下长英质地壳的部分熔融及其后长石、榍石等的分

---

* 本文受"十一·五"国家科技支撑计划项目(2006BAB01A02)和国家自然科学基金项目(41172081)联合资助.
第一作者简介:解洪晶,女,1982 年生,博士生,矿物学、岩石学、矿床学专业,E-mail: xiehongjing717@163.com
** 通讯作者:武广,男,1965 年生,博士,研究员,矿床学和地球化学专业,E-mail: wuguang65@163.com

离结晶作用的产物。结合区域构造演化,本文认为该区钾长花岗岩形成于板内伸展背景。在晚中生代期间,华北板块北缘的构造体制经历了重要的转变,由挤压体制转变为岩石圈减薄和地壳伸展,在伸展体制下,软流圈地幔上涌对上覆长英质地壳的直接加热作用促使其部分熔融形成该区A型花岗岩。

关键词 A型花岗岩;SHRIMP锆石U-Pb年龄;地球化学;道郎呼都格岩体;内蒙古

中图法分类号 P588.121; P597.3

自从Loiselle and Wones(1979)提出以碱性(alkaline)、无水(anhydrous)、非造山(anorogenic)为特征的A型花岗岩以来,引起地质界广泛关注。前人对A型花岗岩的岩石地球化学特征、源区组成、岩石成因及构造背景等已做了较多的研究(Collins *et al.*, 1982; Whalen *et al.*, 1987; Sylvester, 1989; Bonin, 1990; Eby, 1992; Patiño Douce, 1997; Creaser *et al.*, 1991; King *et al.*, 2001)。目前认为,A型花岗岩既可以是过碱的,也可以是准铝或过铝的。Collins *et al.*(1982)和Whalen *et al.*(1987)从常量元素和微量元素地球化学的角度提出了一系列判别指标和图解;Eby(1990, 1992)把A型花岗岩进一步划分为A_1亚型和A_2亚型,并指出A_1亚型指产于与上地幔热柱、裂谷作用有关的非造山环境,A_2亚型主要产出于与大陆边缘地壳伸展作用或与陆内剪切作用产生的拉张环境有关的后造山环境;洪大卫等(1995)则把A型花岗岩划分为AA型(非造山)和PA型(后造山)两类,与Eby的A_1型和A_2型相对应。A型花岗岩的形成包含了多种不同的过程、不同的构造背景以及不同的源区组成,因此对其研究具有重要的地质意义。

中生代期间,华北板块发生了重大的构造转折,构造线方向由EW向转变为NE-NNE向,构造体制也由挤压碰撞转变为大陆伸展,从岩石圈增厚转变为岩石圈减薄。Zhai *et al.*(2007)认为在140~120Ma期间,岩石圈减薄达到顶峰。吴福元和孙德有(1999)认为,在早白垩世时期,华北克拉通东部岩石圈减薄达到了顶峰,局部岩石圈减薄几乎达到了地壳的底部。对华北克拉通内部前寒武纪麻粒岩地体和新生代火山岩的麻粒岩及辉石岩捕虏体的研究发现前寒武纪下地壳与现今下地壳的组成是不同的,也说明华北克拉通发生了下地壳置换和岩石圈减薄(樊祺诚等,2001; 翟明国和樊祺诚,2002)。中生代期间的构造体制的转变及岩石圈减薄事件,导致该区构造岩浆活动强烈,A型花岗岩广泛发育,这些A型花岗岩主要形成于后造山和板内伸展背景(Wu *et al.*, 2002; 陈志广等,2008),为研究A型花岗岩成因及与构造背景关系提供了重要的线索。道郎呼都格A型花岗岩体位于华北克拉通北缘的白乃庙弧内,能为我们研究华北克拉通北缘的构造演化提供新的依据,因此本文拟通过该岩体的岩石学、岩石地球化学和锆石SHRIMP U-Pb定年工作,探讨岩体成因及地球动力学背景。

1 地质背景

道郎呼都格地区位于中亚造山带南缘或华北克拉通北缘白乃庙构造带,属于中亚造山带东段(图1)。中亚造山带形成于古亚洲洋的多阶段俯冲、增生和碰撞作用过程(Dobretsov *et al.*, 1995; Xiao *et al.*, 2004; Windley *et al.*, 2007)。一般认为,东西向索伦缝合带为西伯利亚板块与华北板块的拼合界限(Sengör *et al.*, 1993; Chen *et al.*, 2000),代表了古亚洲洋的最终闭合(Zorin *et al.*, 1993; Xiao *et al.*, 2003)。索伦缝合带与华北克拉通之间为中奥陶-早志留世白乃庙弧和温都尔庙俯冲增生杂岩,它们共同组成华北板块北缘早古生代增生带,古亚洲洋的南向俯冲使该增生带在石炭纪-二叠纪期间演化为安第斯型活动陆缘。索伦缝合带北部增生带由北向南依次为泥盆-石炭纪活动大陆边缘、贺根山蛇绿岩-弧-增生杂岩、晚石炭世宝力道弧-增生杂岩,古亚洲洋的北向俯冲使该增生带在二叠纪演化为安第斯型活动陆缘。在二叠纪晚期,古亚洲洋的最后俯冲使两反向的活动大陆边缘碰撞形成索伦缝合带(Xiao *et al.*, 2003)。

白乃庙弧的基底主要由二云母片岩、角闪-斜长片麻岩和斜长角闪岩组成,其岩性、变质和变形程度与华北板块出露的前寒武纪基底变质岩相当。中部为白乃庙群,广义的白乃庙群包括上部沉积岩系和下部变质火山岩系,前者由凝灰质砂砾岩、硬砂岩和板岩等组成。不整合于沉积岩系之下的是一套变质火山岩(狭义白乃庙群),主要由绿片岩及长英质片岩组成。聂凤军等(1993)获得火山岩系锆石U-Pb年龄为1130Ma,表明白乃庙火山岩系的成岩时代为中元古代。上部为中-上志留统徐尼乌苏组,由浅变质的砂砾岩、千枚岩和结晶灰岩等组成。在这套地层之上不整合覆盖着一套由砂砾岩、硬砂岩夹泥灰岩组成的磨拉石沉积(高计元等,2001)。

区域构造以断裂为主,主要为EW和NE-NNE向两组主要的断裂系统。其中赤峰-白云鄂博断裂是华北板块北缘最重要的EW向断裂,长约600km,宽15~60km。一般认为赤峰-白云鄂博断裂为南部华北克拉通和北部兴-蒙造山带的分界断裂(Davis *et al.*, 2002; Xiao *et al.*, 2003)。其它EW向断裂包括白乃庙弧北部的西拉木伦断裂、林西断裂、锡林浩特断裂、二连浩特断裂以及查干鄂博-阿荣旗断裂。NE-NNE向断裂与中-晚侏罗世太平洋板块的北西向俯冲有关,如大兴安岭主脊断裂、嫩江断裂等(图1)。其中NE-NNE向断裂系统明显比EW向断裂系统年轻(Liu *et al.*, 2010)。区域内海西中晚期、印支期和燕山期岩浆岩广泛发育。海西中晚期及印支期岩浆岩主要沿EW向断裂产出,是古亚洲洋构造域演化的产物,而燕山期的火山、深成岩带与大兴安岭的火山、深成岩带连为一体,主要沿NE-NNE向断裂分布,与环太平洋活动大陆边缘的发育有关(赵越,1994)。

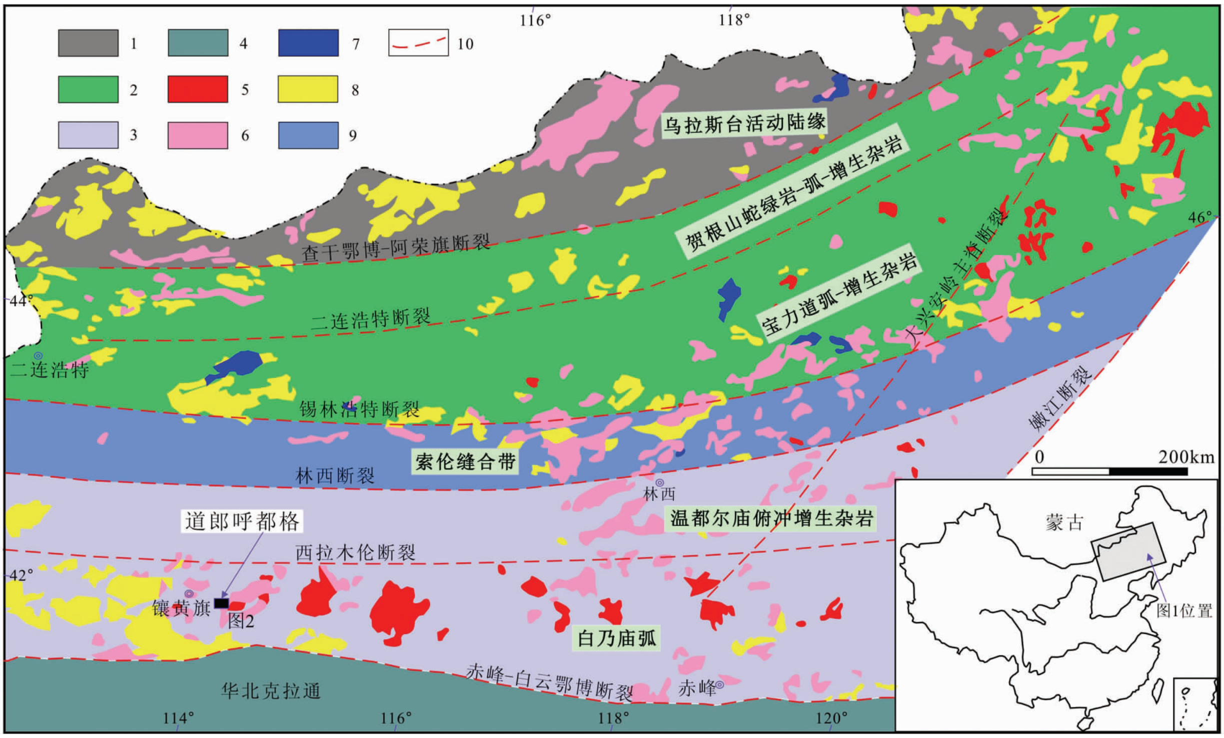

图1　华北克拉通北缘区域地质图(据鲁颖淮等,2009改编)

1-南蒙古生代大陆边缘;2-南蒙古生代弧增生杂岩;3-华北早古生代大陆边缘;4-华北前寒武纪克拉通;5-燕山期浅成岩;6-燕山期深成岩;7-印支期岩浆岩;8-前中生代岩浆岩;9-索伦缝合带;10-断裂

Fig. 1　Sketch regional geological map of the northern margin of the North China Craton (modified after Lu *et al.*, 2009)

1-Paleozoic continental margin of South Mongolia; 2-Paleozoic arc-accretionary complex of South Mongolia; 3-Early Paleozoic continental margin of North China; 4-Precambrian craton of North China; 5-Yanshanian hypabyssal rocks; 6-Yanshanian plutons; 7-Indosinian magmas; 8-Pre-Mesozoic magmas; 9-Solonker suture; 10-fault

2　岩体岩相学特征

道郎呼都格地区位于内蒙古镶黄旗境内,南为赤峰-白云鄂博断裂,北为西拉木伦断裂(图1)。研究区出露地层主要为第三系泥岩、粉砂岩和第四系覆盖物等。区内侵入岩发育,主要由辉长岩、英云闪长岩、二长花岗岩和钾长花岗岩组成(图2),本文主要对钾长花岗岩进行研究,岩体呈不规则状侵位于研究区东南部。钾长花岗岩呈不等粒花岗结构,主要矿物成分有微斜长石、石英、斜长石及黑云母。微斜长石呈粒状,大小在0.3~4.1mm,含量约52%,格状双晶发育,可见交代斜长石现象;石英呈他形粒状,大小在0.1~1.6mm,含量约30%,晶体有裂碎,轻微波状消光(图3a);斜长石半自形板状,大小0.3~3.3mm,含量约16%,发育聚片双晶,并且见其被钾长石和石英交代的现象(图3b);黑云母呈片状,大小在0.2~0.4mm,含量2%,具黑褐-淡黄多色性,有些样品由于风化作用发生褪色而呈淡黄色甚至无色,有的析出铁质而呈黑色。

3　样品采集与分析方法

主量、稀土和微量元素测试由国土资源部廊坊地球物理地球化学勘查研究所完成。其中全岩主量元素采用XRF分析,稀土和微量元素采用ICP-MS分析。主量元素分析精度优于3%,稀土和微量元素分析精度优于5%。

锆石颗粒选自钾长花岗岩样品DH-23,通过常规的重液和磁选进行初选,然后在双目镜下挑出晶形和透明度较好的锆石,将锆石置于环氧树脂中,磨制约一半大小,使锆石内部暴露,用于阴极发光和SHRIMP U-Pb分析。锆石阴极发光在中国地质科学院矿产资源研究所电子探针研究室完成,SHRIMP锆石U-Pb定年在中国地质科学院地质研究所SHRIMP Ⅱ上完成,样品分析流程及原理参见Williams (1998)。应用RSES参考锆石TEM(417Ma)进行元素间的分馏校正,应用SL13(年龄为572Ma,U含量238×10^{-6})标定样品的U、Th和Pb含量。数据处理采用Ludwig SQUID 1.0及ISOPLOT 3.0程序。应用实测^{204}Pb校正锆石中的普通铅,采用年龄为^{206}Pb/^{238}U年龄。

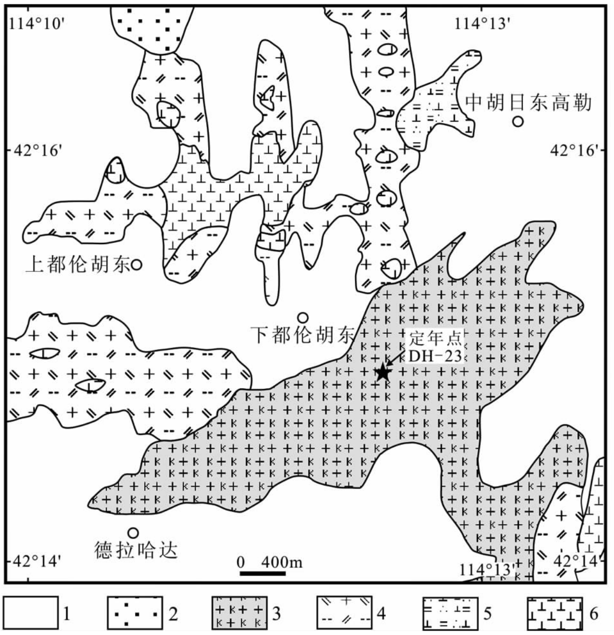

图 2 内蒙古道郎呼都格地区中生代中酸性侵入体及钾长花岗岩分布简图

1-第四系;2-第三系;3-钾长花岗岩;4-二长花岗岩;5-英云闪长岩;6-辉长岩

Fig. 2 Sketch map of Mesozoic intermediate-acid intrusions and K-feldspar granite in Daolanghuduge area, Inner Mongolia

1-Quaternary; 2-Tertiary; 3-K-feldspar granite; 4-monzogranite; 5-tonalite; 6-gabbro

4 分析结果

4.1 锆石 U-Pb 年龄

双目镜下钾长花岗岩的锆石均呈淡黄色,玻璃光泽,透明-半透明,无包体,表面光滑,边界平整,大多呈短柱状,大小 100~150μm,长宽比 1~1.5。阴极发光图像显示出典型的岩浆韵律环带和明暗相间的条带结构(图 4a),属于岩浆结晶的产物。

锆石 SHRIMP 分析结果见表 1。钾长花岗岩样品 DH-23 的 U 和 Th 含量分别介于 $672\times10^{-6}\sim2298\times10^{-6}$ 和 $199\times10^{-6}\sim925\times10^{-6}$ 之间,Th/U 比值介于 0.30~0.58 之间,高于变质成因锆石(一般小于 0.1),而与典型的岩浆成因锆石一致(Williams *et al.*, 1996)。在一致曲线图中,样品数据点分布集中,9 个锆石点的 $^{206}Pb/^{238}U$ 的加权平均年龄为 139.6±1.7Ma,MSWD=0.72(图 4b),指示岩体的结晶年龄。可见,钾长花岗岩形成于早白垩世。

4.2 元素地球化学特征

钾长花岗岩具有较高的 SiO_2(75.79%~78.07%)和 K_2O(4.57%~6.39%),较低的 CaO(0.22%~0.59%)、MgO(0.01%~0.07%)和 TiO_2 含量(0.08%~0.19%)(表 2)。Al_2O_3 含量介于 11.43%~12.50% 之间,铝指数 ASI(ASI=分子数 $Al_2O_3/[CaO+K_2O+Na_2O]$)介于 1.13~1.22 之间,属于过铝质岩石(图 5)。在 QAP 分类图解(图 6a)中,全部落入钾长花岗岩区域,在 SiO_2-K_2O 图解(图 6b)中,投影点都

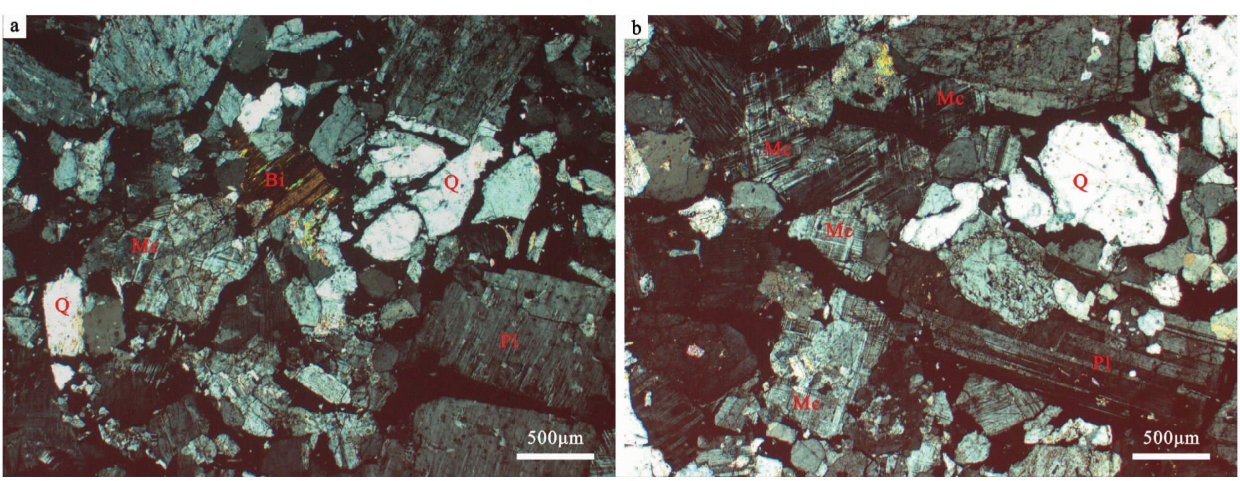

图 3 内蒙古道郎呼都格钾长花岗岩显微结构照片

(a)-钾长花岗岩不等粒结构,石英碎裂现象显著,斜长石聚片双晶发育;(b)-钾长花岗岩不等粒结构,微斜长石格状双晶发育,可见斜长石被钾长石和石英交代现象. Bi-黑云母;Mc-微斜长石;Pl-斜长石;Q-石英

Fig. 3 Photomicrograph showing textural relationships of the Daolanghuduge, Inner Mongolia

(a)-inequigranular texture of K-feldspar granite, displaying fragmentation phenomenon of quartz and polysynthetic twin of plagioclase; (b)-inequigranular texture of K-feldspar granite, showing grid twinning of microcline and metasomatic phenomenon of plagioclase by K-feldspar and quartz. Abbreviations: Bi-biotite; Mc-microcline; Pl-plagioclase; Q-quartz

表 1　道郎呼都格钾长花岗岩 SHRIMP 锆石 U-Pb 分析结果

Table 1　Zircon SHRIMP U-Pb data for the Daolanghuduge K-feldspar granite

测试点	U ($\times10^{-6}$)	Th ($\times10^{-6}$)	$\frac{^{232}Th}{^{238}U}$	$^{206}Pb^*$ ($\times10^{-6}$)	$\frac{^{206}Pb}{^{238}U}$年龄 (Ma)	$\frac{^{206}Pb^*}{^{238}U}$	±%	$\frac{^{207}Pb^*}{^{235}U}$ (%)	±%	$\frac{^{207}Pb^*}{^{206}Pb^*}$ (%)	±%
DH-23-1	1621	845	0.54	30.6	139.6 ±4.1	0.02189	3.0	0.1493	4.1	0.04947	2.8
DH-23-2	2298	925	0.42	42.9	138.3 ±2.4	0.02169	1.7	0.1433	2.6	0.04793	2.0
DH-23-3	882	499	0.58	16.6	139.6 ±2.5	0.02189	1.8	0.1436	2.7	0.04757	2.0
DH-23-4	1186	561	0.49	22.5	140.8 ±2.5	0.02209	1.8	0.1500	3.0	0.04927	2.5
DH-23-5	672	275	0.42	12.4	136.4 ±2.4	0.02138	1.8	0.1509	3.1	0.05119	2.6
DH-23-6	695	199	0.30	13.5	143.7 ±2.5	0.02255	1.8	0.1510	3.9	0.04857	3.4
DH-23-7	1167	583	0.52	21.7	137.6 ±2.4	0.02158	1.8	0.1393	3.4	0.04682	2.9
DH-23-8	1043	405	0.40	19.8	140.3 ±2.4	0.02201	1.8	0.1526	3.5	0.05028	3.0
DH-23-9	873	425	0.50	16.6	140.2 ±2.5	0.02199	1.8	0.1427	4.2	0.04707	3.8

表 2　道郎呼都格钾长花岗岩主量元素(wt%)、稀土及微量元素($\times10^{-6}$)分析结果

Table 2　Major (wt%), rare earth and trace elements ($\times10^{-6}$) compositions of the Daolanghuduge K-feldspar granite

样品号	DH-6	DH-7	DH-8	DH-9	DH-16	DH-17	DH-23	样品号	DH-6	DH-7	DH-8	DH-9	DH-16	DH-17	DH-23
SiO_2	77.89	77.88	77.99	77.44	75.79	76.01	78.07	Er	5.26	5.69	4.88	3.97	4.48	4.13	3.15
Al_2O_3	12.11	12.20	12.18	12.49	12.49	12.50	11.43	Tm	0.90	0.94	0.81	0.67	0.73	0.69	0.56
Fe_2O_3	1.32	1.27	1.30	0.98	2.05	2.03	1.65	Yb	5.68	6.26	5.36	4.25	5.01	4.55	3.74
FeO	0.19	0.15	0.11	0.15	0.28	0.14	0.19	Lu	0.82	0.88	0.78	0.60	0.72	0.68	0.55
MgO	0.03	0.03	0.01	0.03	0.07	0.04	0.03	REE	218.4	298.9	220.9	218.5	346.3	431.5	216.1
CaO	0.24	0.33	0.26	0.35	0.59	0.31	0.22	δEu	0.03	0.03	0.05	0.07	0.12	0.09	0.05
Na_2O	2.65	2.82	2.35	2.66	2.49	1.90	2.05	Sr	17	18	20	14	40	44	14
K_2O	4.86	4.57	5.19	5.14	5.45	6.39	5.68	Rb	251	219	270	294	148	200	303
MnO	0.002	0.001	0.006	0.007	0.020	0.011	0.001	Ba	21	45	78	18	211	135	34
P_2O_5	0.015	0.008	0.011	0.015	0.015	0.019	0.019	Th	45.8	47.5	41.9	60.1	26.4	23.6	61.2
TiO_2	0.09	0.09	0.08	0.08	0.19	0.17	0.08	Nb	39.5	39.6	32.3	37.7	42.4	37.7	33.8
LOI	0.34	0.44	0.45	0.40	0.46	0.45	0.45	Zr	200	190	173	179	417	351	240
Total	99.74	99.80	99.94	99.74	99.91	99.97	99.85	Cs	10.1	11.7	13.8	16.1	11.7	5.7	12.5
A/CNK	1.21	1.20	1.22	1.18	1.13	1.18	1.15	Ga	22.4	23.6	22.4	23.7	24.6	26.6	21.2
$Mg^\#$	4	4	2	4	5	3	3	Hf	8.17	7.94	7.33	7.69	11.98	10.06	8.81
La	31.7	51.2	36.2	40.8	64.8	90.6	43.8	Sc	3.0	3.2	3.4	4.7	3.6	3.1	2.8
Ce	92.2	125.9	87.4	81.6	176.5	208.8	91.2	Cr	2.0	2.0	2.0	2.0	2.0	2.0	2.0
Pr	10.3	14.2	10.9	11.6	14.2	19.8	11.4	V	14	13	14	17	21	18	6
Nd	40.0	54.6	42.6	45.4	50.5	70.9	40.4	Ni	1.5	3.9	1.8	1.8	2.0	4.9	3.6
Sm	9.78	12.72	10.31	10.52	9.57	11.36	7.57	Co	0.5	0.5	0.9	1.0	0.8	1.2	0.3
Eu	0.10	0.12	0.17	0.22	0.36	0.30	0.12	U	2.30	3.16	2.33	3.17	2.69	2.23	2.20
Gd	8.59	11.12	9.04	8.39	8.70	9.57	6.02	Y	51.4	53.9	44.7	37.8	40.5	36.2	24.8
Tb	1.63	2.00	1.60	1.41	1.42	1.43	1.01	Ta	2.21	2.78	2.56	1.90	2.38	2.34	2.30
Dy	9.54	11.22	9.13	7.65	7.76	7.30	5.50	T_{Zr}(℃)	861	852	847	845	921	914	877
Ho	1.88	2.08	1.75	1.45	1.54	1.43	1.08								

位于高钾钙碱性和钾玄岩系列。

稀土元素特征显示钾长花岗岩具有较高的 REE 含量($216.1\times10^{-6}\sim431.5\times10^{-6}$)、轻稀土元素富集、重稀土元素平坦分布特征($(La/Yb)_N=3.76\sim13.42$、$(Gd/Lu)_N=1.30\sim1.75$)。稀土配分曲线呈“海鸥式”分布，δEu 介于 0.03～0.12，具有强烈的铕负异常(图 7a)。

微量元素特征显示钾长花岗岩具有较高的 Rb($148\times10^{-6}\sim303\times10^{-6}$)、Ga($21.2\times10^{-6}\sim26.6\times10^{-6}$)、Zr($173\times10^{-6}\sim417\times10^{-6}$)、Nb($32.3\times10^{-6}\sim42.4\times10^{-6}$)和 Y($24.6\times10^{-6}\sim53.9\times10^{-6}$)含量，较低的 Sr($14\times10^{-6}\sim44\times10^{-6}$)、Ba($18\times10^{-6}\sim211\times10^{-6}$)、Cr(平均 2.0×10^{-6})、Ni(平均 1.5×10^{-6})含量。在微量元素蛛网图上显示强烈

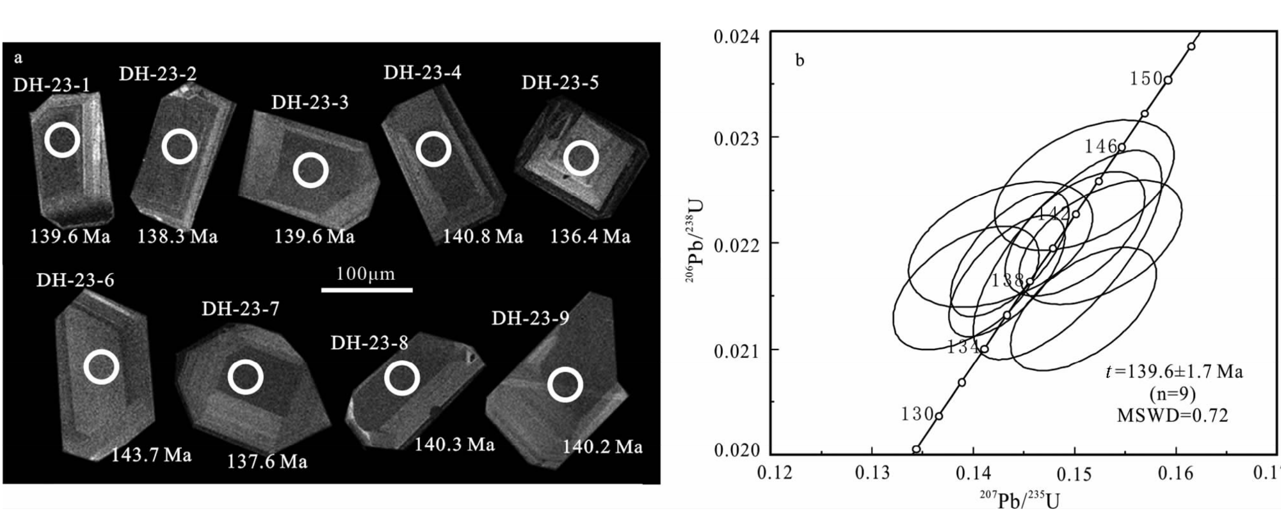

图4 内蒙古道郎呼都格钾长花岗岩锆石形态图(a)及U-Pb年龄谐和图(b)

锆石上的圆圈表示测试点位置

Fig. 4 Cathodoluminescence (CL) images (a) and concordia diagrams of U-Pb zircon dating results (b) from the Daolanghuduge K-feldspar granite, Inner Mongolia

Circles in zircon crystals indicate positions of analytical sites

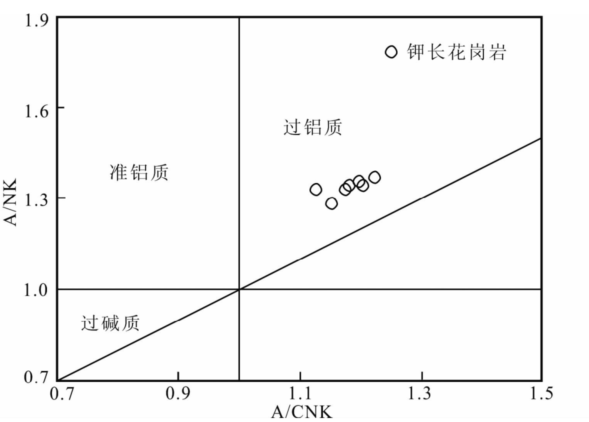

图5 道郎呼都格钾长花岗岩A/NK-A/CNK图解

Fig. 5 A/NK vs. A/CNK plot of the Daolanghuduge K-feldspar granite intrusion

的Ba、Sr、P、Eu、Ti亏损(图7b)。

5 讨论

5.1 岩石属性及成因

A型花岗岩主要的元素地球化学特征是:较高含量的SiO_2、K_2O+Na_2O、Zr、Nb、REE、Y、Ga、F(或Cl)等,较低含量的CaO、Sr、Ba等,较高比值的FeO/MgO、(K_2O+Na_2O)/CaO、Ga/Al等。道郎呼都格钾长花岗岩富硅、富碱、贫钙、高铁镁比值,与A型花岗岩相似,并且具有与A型花岗岩相似的微量元素特征,如较高的Ga、Zr、Nb和Y含量,较低的Sr和Ba含量(Whalen *et al.*, 1987)。10000×Ga/Al比值介于3.48~4.01之间(平均3.64),明显高于I型和S型花岗岩平均值(分别为2.1和2.28),稍低于A型花岗岩值3.75(Whalen *et al.*, 1987)。由于高演化的I、S型花岗岩(SiO_2>74%)的某些特点与A型花岗岩颇为相似,因此利用化学成分准确区分其类型显得尤为重要。王强等(2000)认为,相对于A型花岗岩,高分异S型花岗岩具有更高的P_2O_5含量(均值0.14%),高分异I型花岗岩具有较低的FeO^T含量(<1.00%)和较高的Rb含量(>270×10^{-6})。道郎呼都格钾长花岗岩较低的P_2O_5含量(均值0.014%)区别于高分异的S型花岗岩,较高的FeO^T含量(均值1.54%)和较低的Rb含量(均值241×10^{-6})区别于高分异I型花岗岩。在Whalen *et al.* (1987)提出的判别图解中(图8),所有样品点都投影于A型花岗岩区。因此道郎呼都格钾长花岗岩应属于A型花岗岩。

对于A型花岗岩的成因,一直以来存在着较大争议(Bonin, 2007; Frost *et al.*, 2007),主要观点有(1)地幔碱性岩浆的分离结晶作用(Turner *et al.*, 1992; Mushkin *et al.*, 2003);(2)熔出含水长英质岩浆之后的富F、Cl麻粒岩相下地壳的低程度部分熔融(Collins *et al.*, 1982; Clemens *et al.*, 1986);(3)幔源岩浆与深熔形成的壳源岩浆的混合与交代作用(Harris *et al.*, 1999; Mingram *et al.*, 2000; Yang *et al.*, 2006);(4)低压下钙碱性岩石的部分熔融(Skjerlie and Johnston, 1992; Patiño Douce, 1997)。由于研究区缺乏与钾长花岗岩同时代形成的镁铁质岩石,且钾长花岗岩的SiO_2含量极高并且变化范围较窄,所以幔源岩浆分离结晶机制可能性较小。熔出含水长英质岩浆之后的下地壳麻粒岩相物质的部分熔融也不太可能是本区A型花岗岩的成因机制。实验岩石学研究表明,下地壳麻粒岩物质发生部分熔融后形成富铝贫碱、富镁贫钛的耐熔下地壳,这种残余下地壳物质

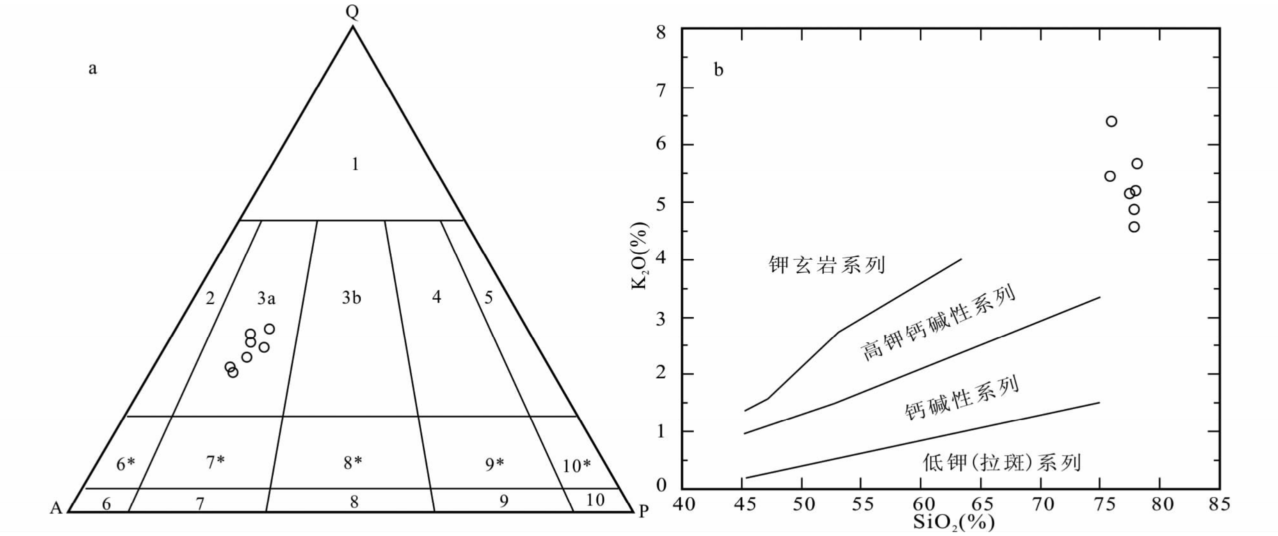

图 6　道郎呼都格钾长花岗岩实际矿物含量 QAP 分类图解（a，据 Streckeisen，1976）和 SiO_2-K_2O 图解（b，据 Peccerillo and Taylor，1976）

Fig. 6　Diagrams of QAP (a, after Streckeisen, 1976) and K_2O vs. SiO_2 (b, after Peccerillo and Taylor, 1976) for Daolanghuduge K-feldspar granite intrusion

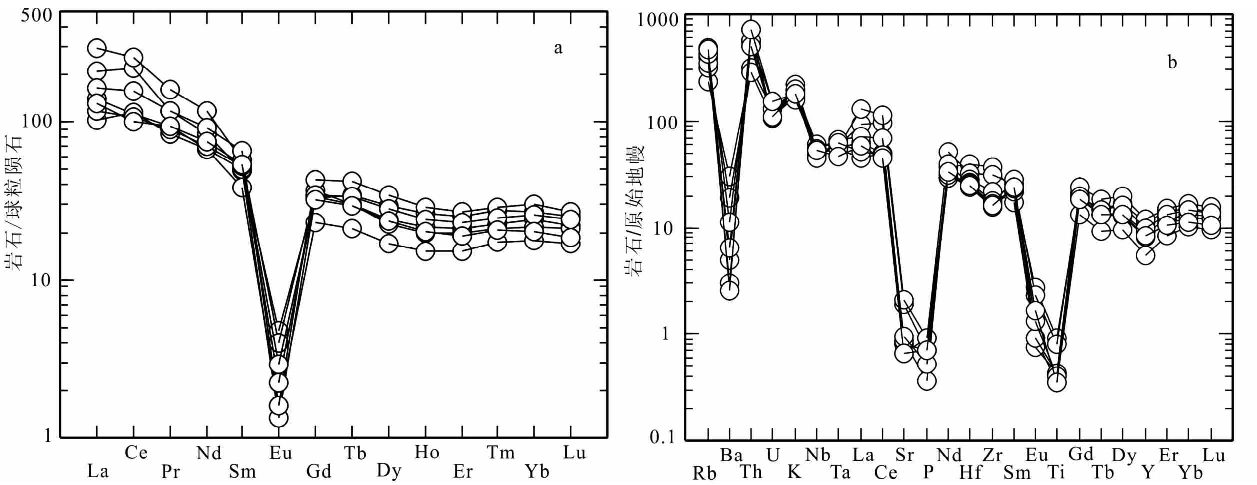

图 7　道郎呼都格钾长花岗岩稀土元素配分曲线（a,标准化值据 Boynton，1984）和微量元素原始地幔标准化蛛网图（b,标准化值据 McDonough *et al.*，1992）

Fig. 7　Chondrite-normalized REE patterns (a, normalization values after Boynton, 1984) and primitive mantle-normalized trace elements spidergrams (b, normalization values after McDonough *et al.*, 1992) of the Daolanghuduge K-feldspar granite

的部分熔融不可能生成 A 型花岗质岩浆（Creaser *et al.*，1991；Patiño Douce，1997）。野外观察显示岩体并不发育镁铁质包体，因此幔源岩浆与地壳熔体的混合成因可能也不是其主要成因机制。A 型花岗岩一般为碱过饱和，而铝不饱和。但越来越多研究表明，A 型花岗岩不仅包括碱过饱和的碱性 A 型花岗岩，还包括准铝、弱过铝、甚至强过铝的铝质 A 型花岗岩（King *et al.*，1997；付建明等，2005）。King *et al.*（1997）认为铝质 A 型花岗岩与碱性花岗岩具有不同的地球化学特征及成因，其中铝质 A 型花岗岩源于具正常水含量的长英质地壳的部分熔融，而碱性花岗岩则为相对“干”的幔源镁铁质岩浆分异的产物。实验岩石学研究表明，英云闪长质-花岗闪长质岩石在浅部地壳的脱水熔融可以形成 A 型花岗岩（Patiño Douce，1997），澳大利亚 Lachlan 褶皱带的铝质 A 型花岗岩即为壳内长英质源岩高温部分熔融形成的（King *et al.*，1997）。道郎呼都格 A 型花岗岩为铝质 A 型花岗岩（图 5），较低的 Al_2O_3 含量（<15%）、强烈亏损的 Sr（Eu）及平坦的 HREE 分布特征（图 7a）指示岩浆形成于富集斜长石且无石榴石残留的浅部低压地区（<10kbar）（Rapp and

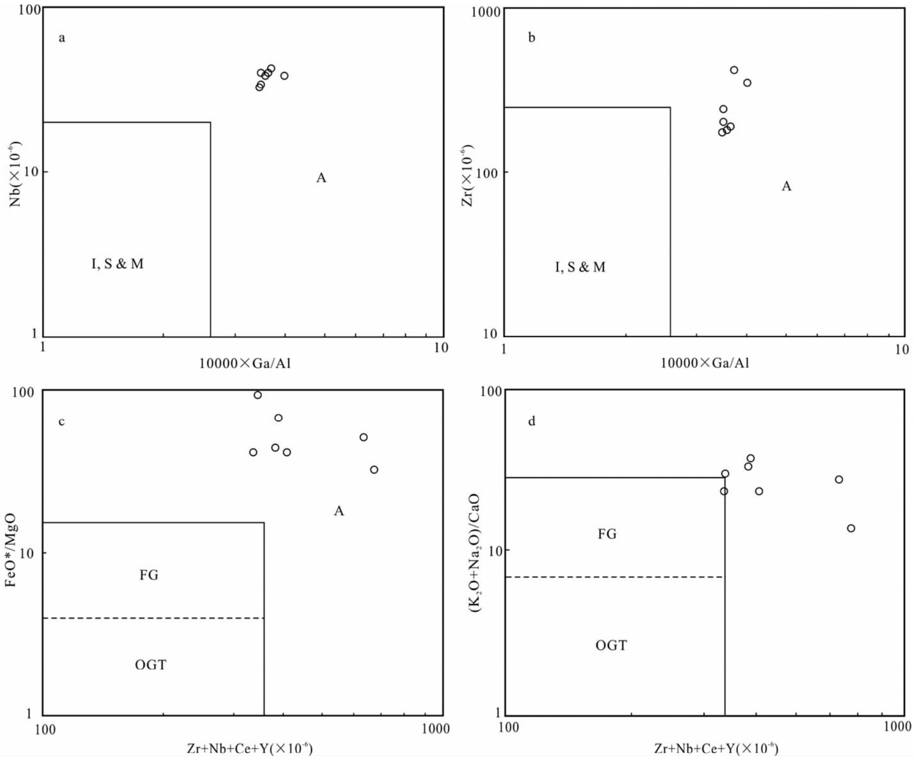

图 8 Nb(a),Zr(b)与 10000 × Ga/Al 判别图和 FeO^*/MgO(c),(K_2O+Na_2O)/CaO(d)与 Zr + Nb + Ce + Y 判别图(据 Whalen *et al.*, 1987)

Fig. 8 Nb (a), Zr (b) vs. 10000 × Ga/Al and FeO^*/MgO (c), (K_2O+Na_2O)/CaO (d) vs. Zr + Nb + Ce + Y discrimination diagrams (after Whalen *et al.*, 1987)

Watson, 1995),所以低压下长英质地壳直接部分熔融及其后的分异作用可能是钾长花岗岩形成的重要机制。由于 A 型花岗岩的 Sr-Nd 同位素测试较困难,本次研究仅获得 1 件样品的 Sr 同位素数据和 3 件样品的 Nd 同位素数据。其 I_{Sr} 值为 0.71123,$\varepsilon_{Nd}(t)$ 值介于 −2.57 ~ −4.66 之间,两阶段 Nd 模式年龄介于 1.14 ~ 1.31Ga。较高的 $\varepsilon_{Nd}(t)$ 值和较年轻的 Nd 同位素模式年龄暗示该 A 型花岗岩的源区不可能为古老的华北克拉通基底物质,而可能为较年轻的地壳物质。在微量元素蜘蛛网图上钾长花岗岩显示强烈的 Ba、Sr、P、Ti 亏损,其中 Sr、Ba 异常可能是斜长石、钾长石分离结晶所致,Ti、P 异常可能是富 Ti 矿物(钛铁矿、榍石等)和磷灰石的分离结晶所致。同时,A 型花岗岩的产生还需要一种高温条件,Clemens *et al.* (1986) 和 Watson and Harrison (1983) 实验显示,$D^{Zr}_{锆石/熔体}$ 分配系数是全岩主成分参数 M = (Na + K + 2Ca)/(Si × Al) 和熔体温度的函数。已知 M 值和全岩 Zr 含量,可计算熔体锆石饱和温度(接近于液相线温度),指示源区最小的岩浆初始温度。道郎呼都格 A 型花岗岩的锆石饱和温度为 845 ~ 921℃,平均 874℃ (n = 7),稍高于澳大利亚 Lachlan 褶皱带铝质 A 型花岗岩的平均值 839℃ (n = 55) (King *et al.*, 1997),明显高于高分异的 I 型花岗岩的形成温度为 764℃ (King *et al.*, 1997)。同时,钾长花岗岩中无继承锆石,这与一般 S 型花岗岩常见继承核不同,也反映了熔体的高温特征。因此,该区钾长花岗岩最有可能为高温低压下长英质地壳部分熔融及其后长石、榍石等的分离结晶作用形成。

5.2 构造背景

A 型花岗岩形成于后造山或非造山环境(Sylvester, 1989; Bonin, 1990; Eby, 1992; Nedelec *et al.*, 1995; Whalen *et al.*, 1996)。Eby(1992)把 A 型花岗岩分为 A_1 和 A_2 两种类型,A_1 型花岗岩侵位于非造山拉张环境,而 A_2 型则侵位于后造山环境。利用 Nb-Y-Ce 及 Y/Nb-Ce/Nb 判别图(图 9),研究区钾长花岗岩样品基本都位于 A_1 型花岗岩区,指示了一种非造山拉张环境。该区钾长花岗岩应属于热花岗岩类型(Miller *et al.*, 2003),该类型花岗岩的产出需要高温热能,与基性岩浆的上侵有关,形成于伸展或转换背景。

华北克拉通北缘从古生代-早侏罗世造山到中侏罗世或早白垩世陆内伸展,经历了漫长的地质演化过程(Meng, 2003; Xiao *et al.*, 2003; Liu *et al.*, 2005)。早古生代,古亚洲洋向华北克拉通俯冲形成早古生代弧增生系列(490 ~ 446Ma)(Xiao *et al.* 2003; Windley *et al.*, 2007),中-晚古生代继续俯冲,在华北克拉通北缘发生安第斯型大陆弧岩浆作

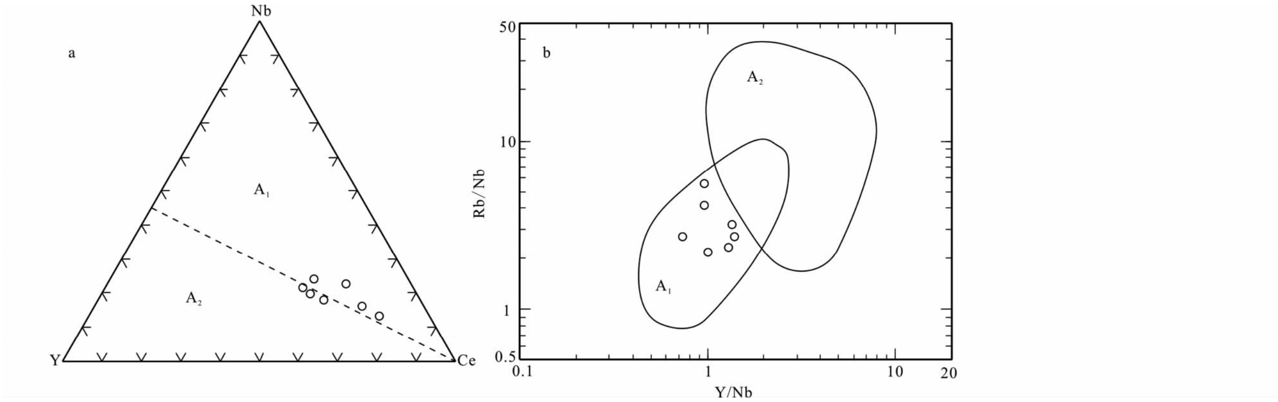

图 9　道郎呼都格钾长花岗岩 Nb-Y-Ce（a）和 Y/Nb-Rb/Nb（b）图解（据 Eby，1992）

Fig. 9　The Nb-Y-Ce (a) and Y/Nb-Rb/Nb (b) diagrams of K-feldspar granite intrusion in Daolanghuduge, Inner Mongolia (after Eby, 1992)

用（390～270Ma；Zhang *et al.*, 2007b, c, 2009）。早中生代，华北克拉通北缘处于局部伸展背景。自印支末期以来，华北板块在继续遭受西伯利亚板块碰撞挤压的同时，古太平洋板块从中侏罗世（约 180Ma）开始向亚洲大陆俯冲（张连昌等，2010），中国东部和华北板块北缘的构造体制经历了重要的转变（赵越，1990），从早中生代的 EW 向构造系统转变为晚中生代的 NE-NNE 向构造系统。之后，中国东部发生岩石圈减薄和地壳伸展（Webb *et al.*, 1999; Davis *et al.*, 2001, 2002; Wu *et al.*, 2002, 2005）。对于伸展作用发生的时间，Wang *et al.*（2004）通过对中蒙边界亚干-翁奇海尔罕（Yagan-Onch Hayrhan）晚中生代花岗岩类研究表明，花岗岩类形成于晚中生代的拉张背景（135Ma）；内蒙古四子王旗钾玄岩是华北板块北缘早白垩世（108～128Ma）岩石圈减薄的直接反映（李毅等，2006）。同时，在晚侏罗-早白垩期间，毗邻地区 A 型花岗岩的广泛分布（Wu *et al.*, 2002）、变质核杂岩的产出（Zheng *et al.*, 1991; Davis *et al.*, 2002）及同期沉积盆地的形成（Graham *et al.*, 2001; Meng, 2003），都指示了一种伸展背景。华北克拉通北缘的碾子沟钼矿区 A 型花岗岩形成于 167Ma，是造山后伸展背景下的产物（陈志广等，2008），而道郎呼都格 A 型花岗岩的产出则指示华北克拉通北缘在 140Ma 时已经进入板内拉张环境。

对于岩石圈减薄的成因机制也是个值得商榷的问题，尽管有多种模式的提出，如热侵蚀作用（Xu *et al.*, 2004; Zheng *et al.*, 2006, 2007）、橄榄岩-熔体相互作用（Zhang, 2005; Zhang *et al.*, 2007a）、岩浆提取作用（Chen et a1., 2004），但拆沉作用是被广泛认可的重要机制（吴福元和孙德有，1999; Gao *et al.*, 2002, 2004; Wu *et al.*, 2005, 2006; 邓晋福等，2006; Deng *et al.*, 2007）。侏罗纪时太平洋板块的俯冲作用，可能使岩石圈受到流体的强烈改造而失去应有的高应变性质，进而导致在早白垩世发生岩石圈拆沉，引发大范围的地壳伸展。Os 同位素资料显示，由地幔橄榄岩包体所反映的新生代岩石圈地幔具有年轻性质，与古生代时的岩石圈地幔截然不同，表明中生代时岩石圈地幔和部分下地壳一起通过拆沉作用而沉入软流圈地幔，由此导致软流圈地幔与地壳的直接接触（吴福元等，2003）。道郎呼都格早白垩世钾长花岗岩最可能形成于拆沉作用引发的拉张环境中，软流圈地幔上涌与地壳直接接触，对上覆长英质地壳的直接加热作用促使其部分熔融形成该区 A 型花岗岩。

6　结论

（1）道郎呼都格钾长花岗岩的锆石 SHRIMP U-Pb 年龄为 139Ma，形成于早白垩世。

（2）道郎呼都格钾长花岗岩富硅、富碱、贫钙、高铁镁比值，具有显著的 Eu 负异常、低 Sr 和 Ba 丰度、以及较高的 Ga、Zr、Nb 和 Y 等元素含量，显示 A 型花岗岩特征，形成于高温低压下长英质地壳的部分熔融及其后长石、榍石等的分离结晶作用。

（3）道郎呼都格钾长花岗岩具有 A_1 型花岗岩的特征，形成于板内拉张背景，是华北克拉通北缘早白垩世岩石圈减薄的产物。

致谢　锆石 SHRIMP U-Pb 定年得到中国地质科学院离子探针中心石玉若博士的帮助；两位审稿人提出了宝贵意见和修改建议；在此致以诚挚的谢意。

References

Bonin B. 1990. From orogenic to anorogenic settings: Evolution of granitoid suites after a major orogenesis. Geological Journal, 25: 261－270

Bonin B. 2007. A-type granites and related rocks: Evolution of a concept, problems and prospects. Lithos, 97: 1－29

Boynton WV. 1984. Cosmochemistry of the rare earth elements: Meteorite studies. In: Henderson P (ed.). Rare Earth Elements Geochemistry. Amsterdam: Elsevier, 63－114

Chen B, Jahn BM, Wilde S and Xu B. 2000. Two contrasting Paleozoic magmatic belts in northern Inner Mongolia, China: Petrogenesis and tectonic implications. Tectonophysics, 328: 157 – 182

Chen B, Jahn BM, Arakawa Y and Zhai MG. 2004. Petrogenesis of the Mesozoic intrusive complexes from the southern Taihang orogen, North China Craton: Elemental and Sr-Nd-Pb isotopic constraints. Contributions to Mineralogy and Petrology, 148: 489 – 501

Chen ZG, Zhang LC, Wu HY, Wan B and Zeng QD. 2008. Geochemistry study and tectonic background of a style host granite in Nianzigou molybdenum deposit in Xilamulun molybdenum metallogenic belt, Inner Mongolia. Acta Petrologica Sinica, 24(4): 879 – 889 (in Chinese with English abstract)

Clemens JD, Holloway JR and White AJR. 1986. Origin of an A-type granite: Experimental constraints. American Mineralogist, 71: 317 – 324

Collins WJ, Beams SD, White AJR and Chappell BW. 1982. Nature and origin of A-type granites with particular reference to Southeastern Australia. Contributions to Mineralogy and Petrology, 80: 189 – 200

Creaser RA, Price RC and Wormald RJ. 1991. A-type granites revisited: Assessment of a residual-source model. Geology, 19: 163 – 166

Davis GA, Zheng YD, Wang C, Darby BJ, Zhang CH and Gehrels GE. 2001. Mesozoic tectonic evolution of the Yanshan fold and thrust belt, with emphasis on Hebei and Liaoning provinces, Northern China. Geological Society of America Memoir, 194: 171 – 197

Davis GA, Darby BJ, Zheng YD and Spell TL. 2002. Geometric and temporal evolution of an extensional detachment fault, Hohhot metamorphic core complex, Inner Mongolia, China. Geology, 30: 1003 – 1006

Deng JF, Su SG, Liu C, Zhao GC, Zhao XG, Zhou S and Wu ZX. 2006. Discussion on the lithospheric thinning of the North China Craton: Delamination? or thermal erosion and chemical metasomatism? Earth Science Frontiers, 13(2): 105 – 119 (in Chinese with English abstract)

Deng JF, Su SG, Niu YL, Liu C, Zhao GC, Zhao XG, Zhou S and Wu ZX. 2007. A possible model for the lithospheric thinning of North China Craton: Evidence from the Yanshanian (Jura-Cretaceous) magmatism and tectonism. Lithos, 96: 22 – 35

Dobretsov NL, Berzin Na and Buslov MM. 1995. Opening and tectonic evolution of the Paleo-Asian Ocean. International Geology Review, 37: 335 – 360

Eby GN. 1990. The A-type granitoids: A review of their occurrence and chemical characteristics and speculations on their petrogenesis. Lithos, 26: 115 – 134

Eby GN. 1992. Chemical subdivision of the A-type granitoids: Petrogenetic and tectonic implications. Geology, 20: 641 – 644

Fan QC, Sui JL, Liu RX and Zhou XM. 2001. Eclogite facies garnet-gyroxenolite xenolith in Hannuoba area: New evidence of magma underplating. Acta Petrologica Sinica, 17(1): 1 – 6 (in Chinese with English abstract)

Frost CD, Ramo OT and Dall'Agnol R. 2007. IGCP project 510: A-type granites and related rocks through time. Lithos, 97: vii – xiii

Fu JM, Ma CQ, Xie CF, Zhang YM and Peng SB. 2005. Ascertainment of the Jinjiling aluminous A-type granite, Hunan Province and its tectonic settings. Geochimica, 34(3): 215 – 226 (in Chinese with English abstract)

Gao JY, Wang YX, Qiu YZ and Zhang Q. 2001. Islands-ocean structural evolution of mid-western continent in Inner Mongulia. Geotectonica et Metallogenia, 25(4): 397 – 404 (in Chinese with English abstract)

Gao S, Rudnick RL, Carlson RW, McDonough WF and Liu YS. 2002. Re-Os evidence for replacement of ancient mantle lithosphere beneath the North China Craton. Earth and Planetary Science Letters, 198: 307 – 322

Gao S, Rudnick RL, Yuan HL, Liu XM, Liu YS, Xu WL, Ling WL, Ayers J, Wang XC and Wang QH. 2004. Recycling lower continental crust in the North China Craton. Nature, 432: 892 – 897

Graham SA, Hendrix MS, Johnson CL, Badamgarav D, Badarch G, Amory J, Porter M, Barsbold R, Webb LE and Hacker BR. 2001. Sedimentary record and tectonic implications of Mesozoic rifting in southeast Mongolia. Geological Society of America Bulletin, 113: 1560 – 1579

Harris C, Marsh JS and Milner SC. 1999. Petrology of the alkaline core of the Messum igneous complex, Namibia: Evidence for the progressively decreasing effect of crustal contamination. Journal of Petrology, 40: 1377 – 1397

Hong DW, Wang SG, Han BF and Jin MY. 1995. Tectonic settings of alkaline granites and their discrimination. Science in China (Series B), 25(4): 418 – 426 (in Chinese)

King PL, White AJR, Chappell BW and Allen CM. 1997. Characterization and origin of aluminous A-type granites from the Lachlan Fold Belt, Southeastern Australia. Journal of Petrology, 38: 371 – 391

King PL, Chappell BW, Allen CM and White AJR. 2001. Are A-type granites the high-temperature felsic granites? Evidence from fractionated granites of the Wangrah Suite. Australian Journal of Earth Sciences, 48: 501 – 514

Li Y, Wu TR, Luo HL and Zhao L. 2006. Geochemistry and tectonic setting of the Early Cretaceous shoshonite of Siziwangqi area, Inner Mongolia. Acta Petrologica Sinica, 22(11): 2791 – 2800 (in Chinese with English abstract)

Liu JM, Zhao Y, Sun YL, Li DP, Liu J, Chen BL, Zhang SH and Sun WD. 2010. Recognition of the Latest Permian to Early Triassic Cu-Mo mineralization on the north margin of the North China block and its geological significance. Gondwana Research, 17: 125 – 134

Liu W, Siebel W, Li XJ and Pan XF. 2005. Petrogenesis of the Linxi granitoids, northern Inner Mongolia of China: Constraints on basaltic underplating. Chemical Geology, 219: 5 – 35

Loiselle MC and Wones DR. 1979. Characteristics and origin of anorogenic granites. The Geological Society of America Abstracts with Programs, 11: 468

Lu YH, Li WB and Lai Y. 2009. Time and tectonic setting of hosting porphyry of the Hadamiao gold deposit in Xianghuangqi, Inner Mongolia. Acta Petrologica Sinica, 25(10): 2615 – 2620 (in Chinese with English abstract)

McDonough WF, Sun SS, Ringwood AE, Jagoutz E and Hofmann AW. 1982. Potassium, rubidium, and cesium in the Earth and Moon and the evolution of the mantle of the Earth. Geochimica et Cosmochimica Acta, 56: 1001 – 1012

Meng QR. 2003. What drove Late Mesozoic extension of the northern China-Mongolia tract? Tectonophysics, 369: 155 – 174

Miller CF, McDowell SM and Mapes RW. 2003. Hot and cold granites? Implications of zircon saturation temperatures and preservation of inheritance. Geology, 31: 529 – 532

Mingram B, Trumbull RB, Littman S and Gertenberger H. 2000. A petrogenetic study of anorogenic felsic magmatism in the Cretaceous Paresis ring complex, Namibia: Evidence for mixing of crust and mantle-derived components. Lithos, 54: 1 – 22

Mushkin A, Navon O, Halicz L, Hartmann C and Stein M. 2003. The petrogenesis of A-type magmas from the Amram Massif, southern Israel. Journal of Petrology, 44: 815 – 832

Nedelec A, Stephens WE and Fallick AE. 1995. The Panafrican stratoid granites of Madagascar: Alkaline magmatism in a post-collisional extensional setting. Journal of Petrology, 36: 1367 – 1391

Nie FJ, Pei RF, Wu LS and Zhang HT. 1993. Magmatic Activity and Metallogeny of the Bainaimiao District, Inner Mongolia, People's Republic of China. Beijing: Beijing Science and Technology Press, 1 – 247 (in Chinese)

Patiño Douce AE. 1997. Generation of metaluminous A-type granites by low-pressure melting of calc-alkaline granitoids. Geology, 25: 743 – 746

Peccerillo A and Taylor SR. 1976. Geochemistry of Eocene calc-alkaline volcanic rocks from the Kastamonu area, northern Turkey. Contributions to Mineralogy and Petrology, 58: 68 – 81

Rapp RP and Watson EB. 1995. Dehydration melting of metabasalt at 8 ~ 32kbar: Implications for continental growth and crust-mantle recycling. Journal of Petrology, 36: 891 – 931

Sengör AMC, Natalín BA and Burtman VS. 1993. Evolution of the Altaid tectonic collage and Paleozoic crustal growth in Eurasis. Nature, 364: 299 – 307

Skjerlie KP and Johnston AD. 1992. Vapor-absent melting at 10kbar of a biotite- and amphibole-bearing tonalitic gneiss: Implications for the generation of A-type granites. Geology, 20: 263 – 266

Streckeisen AL. 1976. Classification of the common igneous rocks by means of their chemical composition: A provisional attempt. Neues Jahrbuch fur Mineralogie, Monatshefte, 1: 1 – 15

Sylvester PJ. 1989. Post-collisional alkaline granites. The Journal of Geology, 97: 261 – 280

Turner SP, Foden JD and Morrison RS. 1992. Derivation of some A-type magmas by fractionation of basaltic magma: An example from the Padthaway Ridge, South Australia. Lithos, 28: 151 – 179

Wang Q, Zhao ZH and Xiong XL. 2000. The ascertainment of Late Yanshanian A-type granite in Tongbai-Dabie orogenic belt. Acta Petrologica et Mineralogica, 19(4): 297 – 306 (in Chinese with English abstract)

Wang T, Zheng YD, Li TB and Gao YJ. 2004. Mesozoic granitic magmatism in extensional tectonics near the Mongolian border in China and its implications for crustal growth. Journal of Asian Earth Sciences, 23: 715 – 729

Watson EB and Harrison TM. 1983. Zircon saturation revisited: Temperature and composition effects in a variety of crustal magma types. Earth and Planetary Science Letters, 64: 295 – 304

Webb LE, Graham SA, Johnson CL, Badarch G and Hendrix MS. 1999. Occurrence, age, and implications of the Yagan-Onch Hayrhan metamorphic core complex, southern Mongolia. Geology, 27: 143 – 146

Whalen JB, Currie KL and Chappell BW. 1987. A-type granites: Geochemical characteristics, discrimination and petrogenesis. Contributions to Mineralogy and Petrology, 95: 407 – 419

Whalen JB, Jenner GA, Longstaffe FJ, Robert F and Gariepy C. 1996. Geochemical and isotopic (O, Nd, Pb and Sr) constraints on A-type granite: Petrogenesis based on the Topsails igneous suite, Newfoundland Appalachians. Journal of Petrology, 37: 1463 – 1489

Williams IS, Buick A and Cartwright I. 1996. An extended episode of early Mesoproterozoic metamorphic fluid flow in the Reynold Region, central Australia. Journal of Metamorphic Geology, 14: 29 – 47

Williams IS. 1998. U-Th-Pb geochronology by ion microprobe. Reviews in Economic Geology, 7: 1 – 35

Windley BF, Alexelev D, Xiao WJ, Kröner A and Badarch G. 2007. Tectonic models for accretion of the Central Asian Orogenic Belt. Journal of the Geological Society, 164: 31 – 47

Wu FY and Sun DY. 1999. The Mesozoic magmatism and lithospheric thinning in eastern China. Journal of Changchun University of Science and Technology, 29(4): 313 – 318 (in Chinese with English abstract)

Wu FY, Sun DY, Li HM, Jahn BM and Wilde S. 2002. A-type granites in northeastern China: Age and geochemical constraints on their petrogenesis. Chemical Geology, 187: 143 – 173

Wu FY, Ge WC, Sun DY and Guo CL. 2003. Discussions of the lithospheric thinning in eastern China. Earth Science Frontiers, 10(3): 51 – 60 (in Chinese with English abstract)

Wu FY, Lin JQ, Wilde SA, Zhang XO and Yang JH. 2005. Nature and significance of the Early Cretaceous giant igneous event in eastern China. Earth and Planetary Science Letters, 233: 103 – 119

Wu FY, Walker RJ, Yang YH, Yuan HL and Yang JH. 2006. The chemical-temporal evolution of lithospheric mantle underlying the North China Craton. Geochimica et Cosmochimica Acta, 70: 5013 – 5034

Xiao WJ, Windley BF, Hao J and Zhai MG. 2003. Accretion leading to collision and the Permian Solonker suture, Inner Mongolia, China: Termination of the central Asian orogenic belt. Tectonics, 22: 1069, doi:10.1029/2002TC001484

Xiao WJ, Zhang LC, Qin KZ, Sun S and Li JL. 2004. Palaeozoic accretionary and collisional tectonics of the eastern Tianshan (China): Implications for the continental growth of Central Asia. American Journal of Science, 304: 370 – 395

Xu YG, Huang XL, Ma JL, Wang YB, Iizuka Y, Xu JF, Wang Q and Wu XY. 2004. Crust-mantle interaction during the tectono-thermal reactivation of the North China Craton: Constraints from SHRIMP zircon U-Pb chronology and geochemistry of Mesozoic plutons from western Shandong. Contributions to Mineralogy and Petrology, 147: 750 – 767

Yang JH, Wu FY, Chung SL, Wilde SA and Chu MF. 2006. A hybrid origin for the Qianshan A-type granite, northeast China: Geochemical and Sr-Nd-Hf isotopic evidence. Lithos, 89: 89 – 106

Zhai MG and Fan QC. 2002. Mesozoic replacement of bottom crust in North China Craton: Anorogenic mantle-crust interaction. Acta Petrologica Sinica, 18(1): 1 – 8 (in Chinese with English abstract)

Zhai MG, Fan QC, Zhang HF, Sui JL and Shao JA. 2007. Lower crustal processes leading to Mesozoic lithospheric thinning beneath eastern North China: Underplating, replacement and delamination. Lithos, 96: 36 – 54

Zhang HF. 2005. Transformation of lithospheric mantle through peridotite-melt reaction: A case of Sino-Korean craton. Earth and Planetary Science Letters, 237: 768 – 780

Zhang HF, Nakamura E, Sun M, Kobayashi K, Zhang J, Ying JF, Tang YJ and Niu LF. 2007a. Transformation of subcontinental lithospheric mantle through peridotitemelt reaction: Evidence from a highly fertile mantle xenolith from the North China Craton. International Geology Review, 49: 658 – 679

Zhang LC, Wu HY, Xiang P, Zhang XJ, Chen ZG and Wan B. 2010. Ore-forming processes and mineralization of complex tectonic system during the Mesozoic: A case from Xilamulun Cu-Mo metallogenic belt. Acta Petrologica Sinica, 26(5): 1351 – 1362 (in Chinese with English abstract)

Zhang SH, Zhao Y, Song B and Liu DY. 2007b. Petrogenesis of the Middle Devonian Gushan diorite pluton on the northern margin of the North China block and its tectonic implications. Geological Magazine, 144: 553 – 568

Zhang SH, Zhao Y, Song B, Yang ZY, Hu JM and Wu H. 2007c. Carboniferous granitic plutons from the northern margin of the North China block: Implications for a Late Paleozoic active continental margin. Journal of the Geological Society, 164: 451 – 463

Zhang SH, Zhao Y, Kröner A, Liu XM, Xie LW and Chen FK. 2009. Early Permian plutons from the northern North China Block: Constraints on continental arc evolution and convergent margin magmatism related to the Central Asian Orogenic Belt. International Journal of Earth Sciences, 98: 1441 – 1467

Zhao Y. 1990. The Mesozoic orogenies and tectonic evolution of the Yanshan area. Geological Review, 36(1): 1 – 13 (in Chinese with English abstract)

Zhao Y. 1994. Geotectonic transition from paleoasia system and paleotethyan system to paleopacific active continental margin in eastern Asia. Scientia Geologica Sinica, 29(2): 105 – 119 (in Chinese with English abstract)

Zheng JP, Griffin WL, O'Reilly SY, Yang JS, Li TF, Zhang M, Zhang RY and Liou JG. 2006. Mineral chemistry of peridotites from Paleozoic, Mesozoic and Cenozoic lithosphere: Constraints on mantle evolution beneath Eastern China. Journal of Petrology, 47: 2233 – 2256

Zheng JP, Griffin WL, O'Reilly SY, Yu CM, Zhang HF, Pearson N and Zhang M. 2007. Mechanism and timing of lithospheric modification and replacement beneath the eastern North China Craton: Peridotitic xenoliths from the 100Ma Fuxin basalts and a regional synthesis. Geochimica et Cosmochimica Acta, 71: 5203 – 5225

Zheng YD, Wang SZ and Wang Y. 1991. An enormous thrust nappe and extensional metamorphic complex newly discovered in Sino-Mongolian boundary area. Science in China (Series D), 34: 1145 – 1152

Zorin YA, Belichenko VG, Turuzantov EK, Kozhevnikov VM, Ruzhentsev SV, Dergunov AB, Filippova IB, Tomurtogoo O, Arvisbaatar N, Bayasgalan T, Biambaa C and Khosbayar P. 1993. The south Siberia-central Mongolia transect. Tectonophysics, 225: 361 – 378

附中文参考文献

陈志广，张连昌，吴华英，万博，曾庆栋. 2008. 内蒙古西拉木伦成矿带碾子沟钼矿区A型花岗岩地球化学和构造背景. 岩石学报，24(4)：879－889

邓晋福，苏尚国，刘翠，赵国春，赵兴国，周肃，吴宗絮. 2006. 关于华北克拉通燕山期岩石圈减薄的机制与过程的讨论：是拆沉，还是热侵蚀和化学交代？地学前缘，13(2)：105－119

樊祺诚，隋建立，刘若新，周新民. 2001. 汉诺坝榴辉岩相石榴辉石岩——岩浆底侵作用新证据. 岩石学报，17(1)：1－6

付建明，马昌前，谢才富，张业明，彭松柏. 2005. 湖南金鸡岭铝质A型花岗岩的厘定及构造环境分析. 地球化学，34(3)：215－226

高计元，王一先，裘愉卓，张乾. 2001. 内蒙古中西部多岛海构造演化. 大地构造与成矿，25(4)：397－404

洪大卫，王式洸，韩宝福，靳满元. 1995. 碱性花岗岩的构造环境分类及其鉴别标志. 中国科学(B辑)，25(4)：418－426

李毅，吴泰然，罗红玲，赵磊. 2006. 内蒙古四子王旗早白垩世钾玄岩的地球化学特征及其形成构造环境. 岩石学报，22(11)：2791－2800

鲁颖淮，李文博，赖勇. 2009. 内蒙古镶黄旗哈达庙金矿床含矿斑岩体形成时代和成矿构造背景. 岩石学报，25(10)：2615－2620

聂凤军，裴荣富，吴良士，张洪涛. 1993. 内蒙古白乃庙地区岩浆活动与金属成矿作用. 北京：北京科学技术出版社，1－247

王强，赵振华，熊小林. 2000. 桐柏-大别造山带燕山晚期A型花岗岩的厘定. 岩石矿物学杂志，19(4)：297－306

吴福元，孙德有. 1999. 中国东部中生代岩浆作用与岩石圈减薄. 长春科技大学学报，29(4)：313－318

吴福元，葛文春，孙德有，郭春丽. 2003. 中国东部岩石圈减薄研究中的几个问题. 地学前缘，10(3)：51－60

翟明国，樊祺诚. 2002. 华北克拉通中生代下地壳置换：非造山过程的壳幔交换. 岩石学报，l8(1)：1－8

张连昌，吴华英，相鹏，张晓静，陈志广，万博. 2010. 中生代复杂构造体系的成矿过程与成矿作用——以华北大陆北缘西拉木伦钼铜多金属成矿带为例. 岩石学报，26(5)：1351－1362

赵越. 1990. 燕山地区中生代造山运动及构造演化. 地质论评，36(1)：1－13

赵越. 1994. 东亚大地构造发展的重要转折. 地质科学，29(2)：105－119